Appl. Phys. B 74 [Suppl.], S171–S176 (2002)
DOI: 10.1007/s00340-002-0881-0

Applied Physics B
Lasers and Optics

Z. WEI[1,2,✉]
Y. KABOYASHI[3]
K. TORIZUKA[3]

Passive synchronization between femtosecond Ti:sapphire and Cr:forsterite lasers

[1] New Energy and Industrial Technology Development Organization, 3-1-1 Higashi-Ikebukuro, Tokyo 170-6027, Japan
[2] Laboratory of Optical Physics, Institute of Physics and Center of Condensed Matter Physics, Chinese Academy of Sciences, Beijing 100080, P.R. China
[3] Institute of Photonics, National Institute of Advanced Industrial Science and Technology, 1-1-4 Umezono, Tsukuba, Ibaraki 305-8568, Japan

Received: 15 September 2001 /
Revised version: 1 November 2001
Published online: 27 June 2002 •

ABSTRACT Two independent femtosecond Ti:sapphire and Cr:forsterite lasers were stably synchronized by crossing both lasers inside the Ti:sapphire crystal. We obtained two-color femtosecond pulse trains at the completely different wavelengths of around 820 nm and 1250 nm respectively. This new technique overcomes the gain competition and enables us to greatly broaden the tunable ranges. By optimizing the overlap of the beams, we realized a large tolerance of cavity-length mismatch of 5 μm and demonstrated long-term synchronization that continuously remained over several hours. The measured FWHM of the cross-correlation trace is 74 ± 2 fs based on the 43 ± 2-fs Ti:sapphire and 52 ± 1-fs Cr:forsterite lasers. The exact coincidence with the theoretical calculated value infers the two-color laser being synchronized with a timing jitter of only a few femtoseconds.

PACS 42.60.Fc; 42.60.By; 42.65.Re

1 Introduction

The technology of Kerr-lens mode locking (KLM) in solid-state lasers has greatly pushed the development of femtosecond science. Up to now, the Ti:sapphire and Cr:forsterite lasers have been demonstrated as the two successful examples among the available KLM lasers. By inducing the intra-cavity self-phase-modulation (SPM) effect, recently C. Chudoba et al. [1] and R. Ell et al. [2] directly generated few-cycle pulses from both lasers with ultra-broadband spectra. Obviously, synchronizing the above lasers will give us a potential to produce two-color femtosecond pulses in unprecedented bandwidths and pulse durations. Such a laser will be an ideal tool as the frequency comb for the measurement of absolute optical frequency in metrology [3].

Previous two-color femtosecond solid-state lasers, using either active synchronization with an electrical feedback device [3–5] or passive synchronization by the nonlinear coupling effect, used only a Ti:sapphire crystal as the gain medium [6–11]. Because of the single gain medium, the latter laser suffered from limited bandwidths, poor tunability and close optical frequencies.

✉ Fax: +81-298-615102, E-mail: z.wei@aist.go.jp

In this paper, we present a novel passive technique of synchronizing two different femtosecond lasers based on the nonlinear coupling mechanism between Ti:sapphire and Cr:forsterite lasers. By crossing both lasers inside the Ti:sapphire crystal, we obtained two-color femtosecond pulse trains at the completely different wavelengths of around 820 nm and 1250 nm. This design overcomes the gain competition and gives us a potential of broadening the bandwidths and tunability. Compared to the active synchronization with electrical feedback scheme, the passive technique was stimulated by cross-phase modulation (XPM) and should be capable of operating at lower fluctuation, which will result in a very small timing jitter.

The mechanism of passive synchronization can be attributed to the XPM effect between two coupled femtosecond KLM lasers. Considering the lasers to operate at the repetition rates of f_1 and f_2 respectively, before the synchronization occurs, they cross in the Kerr medium at a repetition rate of $f_1 - f_2$ and suffer the instantaneous frequencies of ω_1 and ω_2:

$$\omega_1 = \omega_{01} - n_2(\omega_{01}, \omega_{01}) \frac{\partial I_1}{\partial t} - n_2(\omega_{01}, \omega_{02}) \frac{\delta}{v_2} \frac{\partial I_2}{\partial t} \quad (1)$$

$$\omega_2 = \omega_{02} - n_2(\omega_{02}, \omega_{02}) \frac{\partial I_2}{\partial t} - n_2(\omega_{02}, \omega_{01}) \frac{\delta}{v_1} \frac{\partial I_1}{\partial t} \quad (2)$$

Here $I_i (i = 1, 2)$ is the intra-cavity laser intensity, ω_{0i} is the central frequency, $n_2(\omega_{01}, \omega_{01})$ and $n_2(\omega_{02}, \omega_{02})$ are the SPM nonlinear indexes for laser 1 and laser 2 respectively, $n_2(\omega_{01}, \omega_{02})$ is the XPM nonlinear index, v_i is the mode volume and δ is the overlap volume between the two lasers. Considering the instant of time when both laser pulses start to cross, for the case of laser 1 behind laser 2, the leading part of laser 1 crosses with the trailing part of laser 2. From (1) and (2), we easily deduce that the spectrum of laser 1 is shifted into the blue because of the negative slope of intensity I_2 in the trailing pulse, and laser 2 is shifted into the red because of the positive slope of intensity I_1 in the leading pulse. In the laser cavities with negative group dispersions, the round-trip time of laser 1 will decrease but that of laser 2 will increase. If both cavity lengths have been adjusted to be nearly equal, the time interval of both laser pulses inside the Kerr medium will be shortened after one round trip and the next crossing will be further enhanced in the time domain. Therefore, the time in-

terval will become shorter and shorter, until both laser pulses maximally overlap in the time domain. Vice versa, if the laser 1 is ahead of the laser 2, the crossing will happen at the trailing part of laser 1 and the leading part of laser 2; which leads laser 1 and laser 2 in red and blue shifts respectively. So, we once again deduce that laser 2 will speed up and laser 1 will slow down corresponding to the times of the round trip in the cavities with negative group dispersions, resulting in both laser pulses also being maximally overlapped.

Once both laser pulses are maximally overlapped, the shifts of carrier frequency vanish because of the symmetrical spectral broadening and both pulses operate at the same round-trip time. For any minor jitter between the two pulses arising from noise and environmental perturbations, due to the above dynamics process the pulses can automatically maximally overlap again after enough round trips. This behavior corresponds to a pulling effect of two laser pulses on each other; in this case both pulses are locked together and the laser performs a synchronized operation.

2 Experimental setup

We synchronized the femtosecond KLM Ti:sapphire and Cr:forsterite lasers by coupling both laser pulses in the Ti:sapphire crystal. This design is based on two reasons: (i) the Ti:sapphire crystal is transparent for the Cr:forsterite laser and (ii) the high nonlinear index n_2 is expected in the Ti:sapphire crystal. A schematic of the novel two-color femtosecond laser is shown in Fig. 1. It consists of a prism dispersion controlled KLM Ti:sapphire laser and a self-starting KLM Cr:forsterite laser. The gain media are Ti:sapphire and Cr:forsterite crystals with the lengths of 4 mm and 7 mm respectively. Both of them were set at Brewster angles and maintained at the temperatures of 11 °C and 1 °C respectively. The Cr:forsterite crystal was also covered in a small plastic box and purged by flowing nitrogen to keep the surface dry. In order to induce a stronger XPM effect for synchronization by beam crossing with a narrower angle, we used two pairs of D-shaped concave mirrors around the Ti:sapphire crystal and set the mirrors at the gaps of less than 1 mm by using independent mirror mounts. Where M1 and M2 were the focus mirrors for the Ti:sapphire laser, M3 and M4 were inserted into the Cr:forsterite laser cavity for introducing an additional focal point inside the Ti:sapphire crystal. This design greatly enhances the coupling between two laser beams with the standard commercial mirrors. For reliable KLM of the Cr:forsterite laser [12], a broadband SESAM (semiconductor saturable-absorber mirror) was used as the end mirror. A pair of fused-silica prisms (P1 and P2) and a pair of SF6 prisms (P3 and P4) were used to compensate the dispersion inside the respective cavities. Considering the basic condition of synchronizing lasers, we set both cavities at the same length. A piezo-transducer (PZT) was also used to drive the end mirror M8 in the Ti:sapphire laser to fine tune the match of cavity lengths between the two lasers. To measure the cross correlation easily in the latter, the lengths of the two arms from the Ti:sapphire crystal to output couplers of T1 and T2 were aligned as close as possible. An orange glass filter was placed behind the coupler T1 to block the remaining pump laser. After reflection by two pairs of mirrors, both Ti:sapphire and Cr:forsterite lasers were input to the auto correlators and cross correlator for the measurement of pulse durations and the cross-correlation trace.

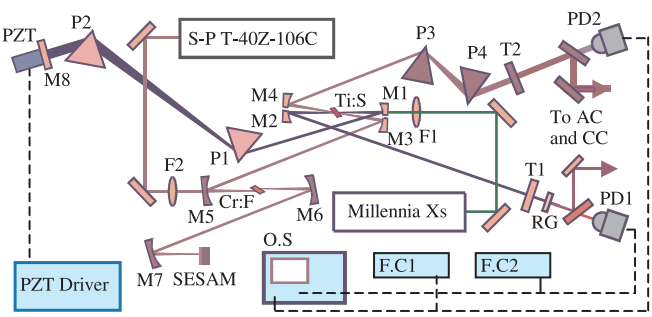

FIGURE 1 Experimental setup. Both Ti:sapphire and Cr:forsterite lasers are coupled inside the Ti:sapphire crystal by half-cut mirrors M1 to M4. M1–M6: CVI TLM2 mirrors with ROC of 10 cm and diameter of 0.5 in; M7: HR with ROC of 20 cm and diameter of 1 in; M8: mini-plate HR with 10-mm diameter × 1-mm thickness; T1 and T2: output couplers with transmissivities of 5% and 3% ; P1 and P2: fused-silica prisms; P3 and P4: SF6 prisms; PD1 and PD2: fast photodiodes; PZT: piezo-transducer; RG: orange glass filter; AC: auto correlator; CC: cross correlator. F.C1. and F.C2.: frequency counters; O.S.: oscilloscope; M3–M7 and T2 were coated at 1300 nm, others were coated at 850 nm

We pumped the Ti:sapphire and Cr:forsterite lasers with the all-solid-state 532-nm (S-P Inc., Millennia Xs) and 1.06-μm lasers (S-P Inc., T-40Z-106C) respectively. Both pump sources are diode-pumped Nd : YVO_4 lasers. Under the pump powers of 5 W at the 532-nm laser and 9 W at the 1.06-μm laser, we obtained the stable KLM powers of about 600 mW and 110 mW from the Ti:sapphire and Cr:forsterite lasers respectively. The distance between the beam spots on two close D-shaped mirrors (M2 and M4) was about 3 mm. No obvious power reduction was observed in the Cr:forsterite laser compared to the standard configuration with five mirrors. By changing the inserted material of the prisms, we obtained the shortest pulses as 11 fs and 40 fs from each laser.

3 Results and discussion

3.1 *Observation of synchronization*

To observe the synchronization between the Ti:sapphire and Cr:forsterite lasers, we first used two frequency counters (HP 53132A) to measure the repetition rates of both KLM lasers. By fine tuning the cavity length of the Ti:sapphire laser, the repetition rates can be set at the same values; covering the lasers with a closed box to prevent air turbulence enables repetition rates with an accuracy of $1 \pm$ Hz and no obvious drift within one minute. Then, an oscilloscope (HP 54616B) was used to monitor the pulse trains of both lasers; triggering using one pulse train allows the other pulse train to be viewed. Before successful synchronization, the other pulse train could not be clearly displayed on the oscilloscope. Although the repetition rates were tuned to exactly the same values with the aid of frequency counters, slips of the trace were always observed due to the existing environmental perturbations (Fig. 2a). We considered this as failed synchronization due to weak coupling between the two pulses.

By aligning the overlap between two laser beams inside the Ti:sapphire crystal and re-driving the PZT again to fit the match of the cavity lengths, we found that the pulse trains

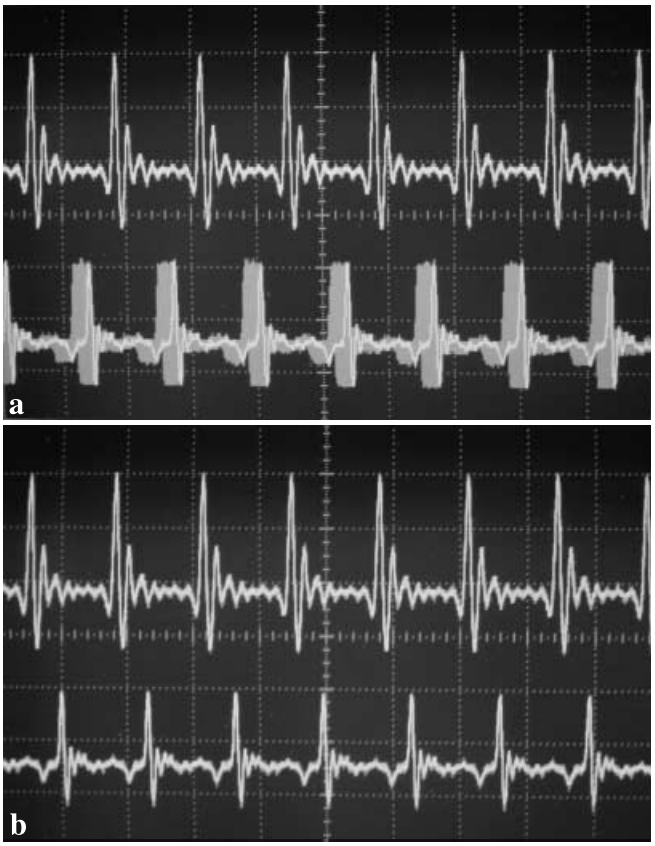

FIGURE 2 The pulse traces of Ti:sapphire (*top*) and Cr:forsterite (*bottom*) lasers at the modes of free running (**a**) and synchronization (**b**). The oscilloscope was triggered by the Ti:sapphire laser and set at 10 ns/div. Both repetition rates have been pre-set at the same values. In (**a**) the pulse trains of the Cr:forsterite laser shows the slip of the trace due to the environmental perturbations before success in synchronization. The traces in (**b**) show the pulse locking when synchronization occurs

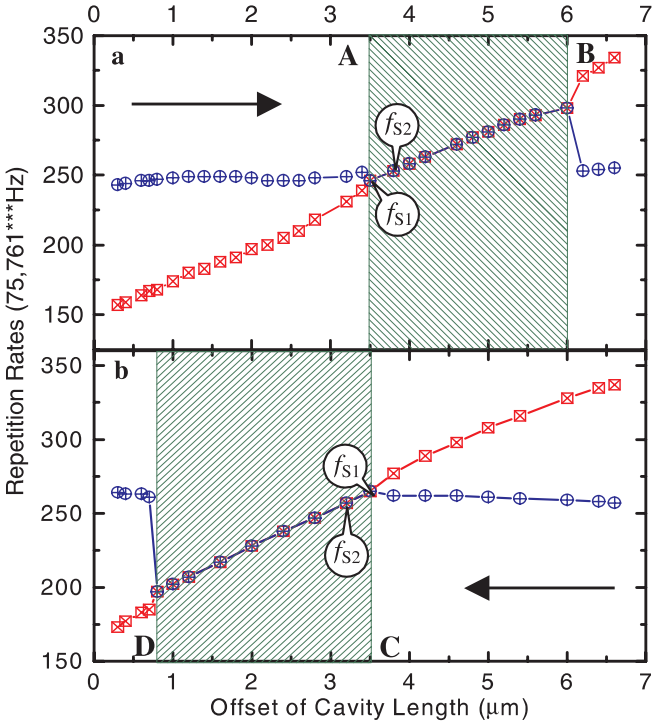

FIGURE 3 The repetition rates of the Ti:sapphire (*normal cross squares*) and Cr:forsterite (*slope cross circles*) lasers versus the offset of cavity length by shortening (**a**) and lengthening (**b**) the cavity length of the Ti:sapphire laser. The synchronization occurs in the range (*shade*) from A (C) to B (D). f_{S1} is the locked repetition rate at the critical positions of starting synchronization, f_{S2} is that at the next positions. To easily scale the ordinate we subtracted 75.761000 Hz from the exact repetition rate

were locked together when both repetition rates tended to be the same. The repetition rate of the Cr:forsterite laser jumped to the same value as that of the Ti:sapphire laser and then the oscilloscope showed the stable trace as shown in Fig. 2b. Even if we continuously changed the repetition rate of the Ti:sapphire laser by tuning the PZT, the pulse locking still remained, until further driving the PZT collapsed the lock; then the pulse-train trace of the Cr:forsterite laser displayed slip again. This phenomenon reflected the typical synchronization between the Ti:sapphire and Cr:forsterite lasers.

Figure 3 shows the behaviors of the repetition rates of Ti:sapphire (squares) and Cr:forsterite (circles) lasers when the PZT is extended (in Fig. 3a, the cavity length is decreased) and shortened (Fig. 3b) respectively. The horizontal scales are shifts of the end mirror M8 driven by the PZT; the repetition rates are plotted on the vertical coordinate axis. At the beginning both lasers worked at the different round-trip frequencies independently; adjusting the displacement of M8 via the PZT will change the repetition rate of the Ti:sapphire laser. When the repetition rate of the Ti:sapphire laser is close enough to that of the Cr:forsterite laser, the Cr:forsterite laser will be captured by the Ti:sapphire laser and then forced to follow the repetition rate determined by the cavity length of the Ti:sapphire laser. It reveals a master–slave behavior within the regime of synchronization, until out of the tolerance region of cavity-length mismatch. Then the Cr:forsterite laser returned to its initial repetition rate and was independent of the further shift of the PZT. In general, this feature was explained as the higher power and shorter pulse duration of the Ti:sapphire laser. Since the Ti:sapphire laser induces a stronger nonlinear effect on the Cr:forsterite laser than the Cr:forsterite laser on the Ti:sapphire laser, this results in the Cr:forsterite laser being pulled to match the repetition rate of the Ti:sapphire laser. In fact, although the Cr:forsterite laser causes a weaker nonlinear effect, it still should affect the feature of the Ti:sapphire laser. We present further experimental results and an explanation in Sect. 3.2.

With the optimized coupling of two laser pulses inside the Ti:sapphire crystal and the suitable pulse durations, we observed that the synchronization occurred when the difference in the repetition rates was close to about 15 Hz (around the starting positions A and C). Further, a long tolerance of cavity-length mismatch over 2.5 μm was demonstrated. The difference in repetition rates was over 60 Hz out of the synchronized regime (around the end positions B and D) by continuously tuning the cavity length via the PZT. In general, driving the PZT in the reverse direction showed similar behaviors except for a backward shift of the synchronized regime. Although we measured both synchronized regimes partly overlapped in the initial experiment, our recent work showed the reversed synchronization normally occurred around the starting position (A) of the first synchronized regime. When driving the PZT oppositely before the end position B (or D), we found that the synchronization almost covered both regimes, until

the mirror M8 shifted around the end position D (or B) in the reversed synchronized regime, corresponding to a total tolerance of about 5 μm. The long-term synchronized operation maintained over many hours was also obtained by shifting M8 in the middle region of the synchronized regimes.

3.2 *Wavelength towing and tuning*

Under the synchronized mode, we observed that both laser wavelengths were shifted relative to each other in opposite directions as the end mirror M8 was driven via the PZT [13]. Figure 4 shows the measured results when we scanned the offset of cavity length over the synchronized regimes. Compared to the measurement of repetition rates, a bigger error existed in estimating the central wavelength because of the resolution of spectrometers for broadband spectra. However, the measured data still well revealed the unique feature of wavelength towing in the synchronized regime [14]. Different to the result in the pure two-color femtosecond Ti:sapphire lasers [15], our experiment showed that both wavelengths were affected by the coupling process. In fact, this feature can be explained with the XPM mechanism.

For our discussion, we denote the repetition frequencies of free-running Ti:sapphire and Cr:forsterite lasers as f_{Ti} and f_{Ci}, where $i = 1, 2$ correspond to the notation in Fig. 3. When we shorten the cavity length by moving the end mirror M8 to the critical position A for synchronization (Fig. 4a),

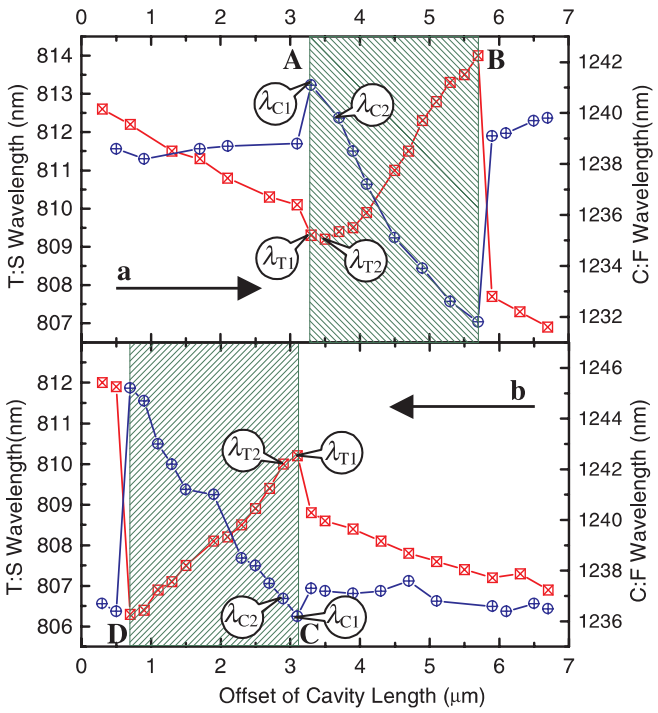

FIGURE 4 The wavelengths of the Ti:sapphire (*normal cross squares*) and Cr:forsterite (*slope cross circles*) lasers versus the offset of cavity length by shortening (**a**) and lengthening (**b**) the cavity length of the Ti:sapphire laser. Because of the increasing nonlinear coupling effect, the wavelengths of both lasers were shifted to λ_{T1} und λ_{C1} respectively at the critical positions A and C for synchronization. Further changing the cavity length will reverse shift the two wavelengths to λ_{T2} und λ_{C2} respectively for pulse locking. The XPM effect vanished from the synchronized regime and led to both lasers freely operating at the original wavelengths

an occasional overlap between two laser pulses in the Ti:sapphire crystal will start the synchronization. After the next round trip, the Ti:sapphire laser pulse will arrive at the crystal behind the pulse of the Cr:forsterite laser because of its slightly lower repetition rate f_{T1} than f_{C1}. Then, the nonlinear coupling will occur at the leading and trailing Ti:sapphire and Cr:forsterite laser pulses respectively. In this case the former should be blue-shifted to wavelength λ_{T1} and the latter should be red-shifted to λ_{C1}. Considered the negative group dispersion inside laser cavities, the repetition rate f_{T1} will increase and f_{C1} will decrease, resulting in them evolving to the same value f_{S1} ($f_{T1} < f_{S1} < f_{C1}$) and then being locked together. With the further shortening of its cavity length, the Ti:sapphire laser has a potential to be operated at a bigger repetition rate f_{T2}, so that its pulse is going to be ahead of the Cr:forsterite laser pulse. In this situation the opposite wavelengths shift (λ_{T2} and λ_{C2}) compared to the coupling process at the critical position A, resulting in both lasers once again evolving to a new common repetition rate f_{S2}. When continuously tuning the cavity length, not only the repetition rates, but also the wavelengths, showed similar behaviors and shifted reasonably, until they left the end position B of the synchronized regime where the XPM effect can not compensate the difference from the free-running one any more. Above the critical point, both lasers operated independently again and operated at the free-running wavelengths. Vice versa, by lengthening the cavity length, the synchronized lasers showed the opposite shift in wavelengths with a similar mechanism (Fig. 4b).

The behaviors of both repetition rates observed in Fig. 3 are also consistent with the above explanation of the XPM mechanism. Compared to the normal free-running mode, we clearly found that the repetition rate of the Ti:sapphire laser was varied at an increasing slope as the displacement of M8 was close to the synchronizing border A (or C). The reason is that the increasing nonlinear effect gradually plays a significant role for the repetition rate of the Ti:sapphire laser besides the cavity length changing during this process. With the increasing nonlinear effect, the repetition rate of the Cr:forsterite laser was also shifted at the same time. When the cavity length was tuned at the critical position A (or C), the nonlinear coupling effects between the two lasers were capable of evolving their repetition rates (f_{T1} and f_{C1}) to the same one (f_{S1}) and then they locked the two repetition rates together. Within the synchronized regime, both laser pulses cross in the opposite parts as the cavity-length tuning, so that the locked repetition rate varied at a smaller slope than that in the free-running mode, until they arrive at the end border B (or D). Once further tuning the cavity length has collapsed the synchronization, we can see the sudden recovery of both repetition rates to the values in the free-running mode. In view of the above analysis, we consider the contribution of the Ti:sapphire laser was not so strictly dominant in the synchronization, in spite of its master-like behavior on the repetition rate. In the synchronized operation, the values of the locked repetition frequency and the laser wavelengths should be balanced with both lasers. Not only the power and pulse width of each laser, but also the intra-cavity dispersion of the lasers, should affect the values.

By changing the insertion of two prisms, we could tune the corresponding laser wavelengths independently. Figure 5

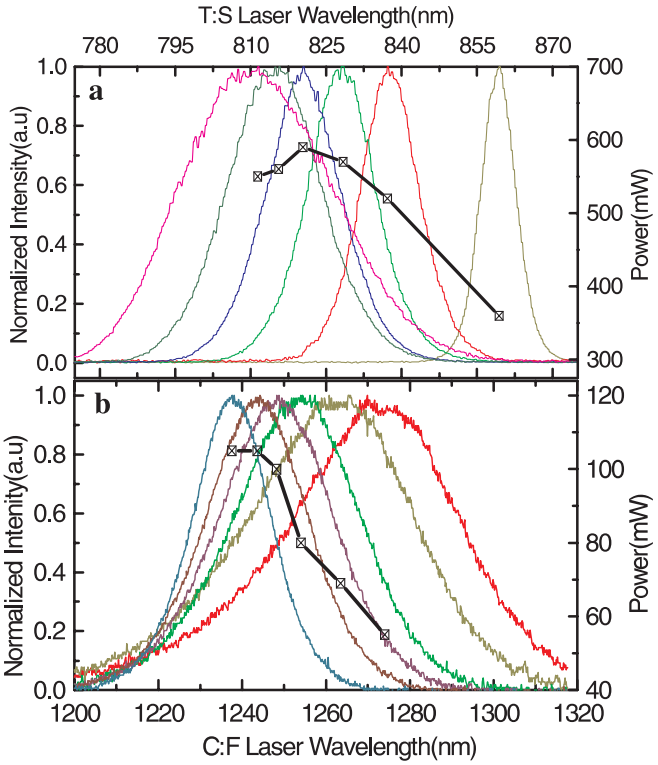

FIGURE 5 The tuning characteristics for synchronized operation of the Ti:sapphire (**a**) and Cr:forsterite (**b**) lasers. Both output powers versus their wavelengths were plotted as the *cross square lines*. The normalized spectra for both lasers showed the characteristic of bandwidth versus wavelengths

shows the tunable ranges of both laser branches with synchronizing mode, which were limited by the lower laser power in the longer-wavelength side and bandwidths of the mirrors (whose center wavelengths are 850 nm and 1300 nm) in the shorter-wavelength side, respectively. For the Ti:sapphire laser, the maximum output power was 590 mW around the central wavelength of 820 nm and that for the Cr:forsterite laser was 105 mW around 1250 nm. We measured that the pulse widths of both lasers are inversely proportional to their bandwidths. Although the shortest pulses appeared at the central wavelengths around 810 nm and 1280 nm respectively, synchronizing lasers under those situations showed the shorter tolerance of cavity-length mismatch.

3.3 *Measurement of cross correlation*

To measure the cross correlation, we aligned the synchronized lasers operated with the best stability and a long tolerance of cavity-length mismatch. A home-made cross correlator was used to measure the correlation trace between the Ti:sapphire and Cr:forsterite lasers (Fig. 6). After passing through a variable delay line with the PZT-controlled roof reflector, the Ti:sapphire laser beam was overlapped with the Cr:forsterite laser beam on the metal beam splitter (B.S.). The co-linear beams of both lasers were focused in the nonlinear crystal BBO to generate the sum-frequency signal (SFG). After the collimating with the second lens, a grating was used to separate the SFG and two SHG signals generated by the Ti:sapphire and Cr:forsterite lasers respectively. This setting enables us to catch easily the cross signal with the eyes. By

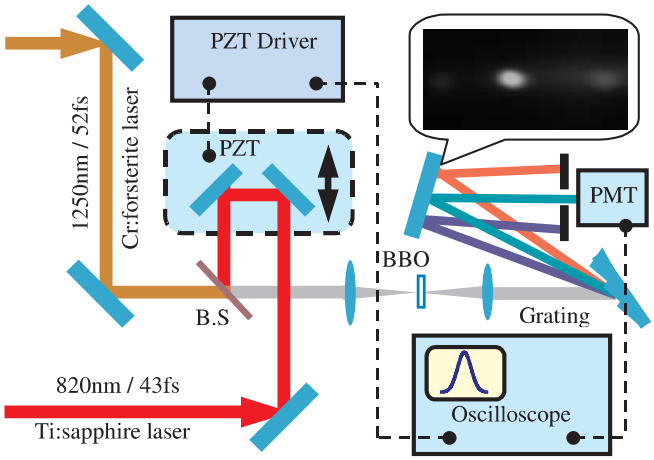

FIGURE 6 Schematic of the configuration for measurement of the cross-correlation traces. B.S.: metal beam splitter. The *inset picture* shows the beam patterns dispersed with the grating. The green one in the *middle* is the SFG between the two lasers. The blue and red ones are the SHG of the Ti:sapphire and Cr:forsterite lasers respectively

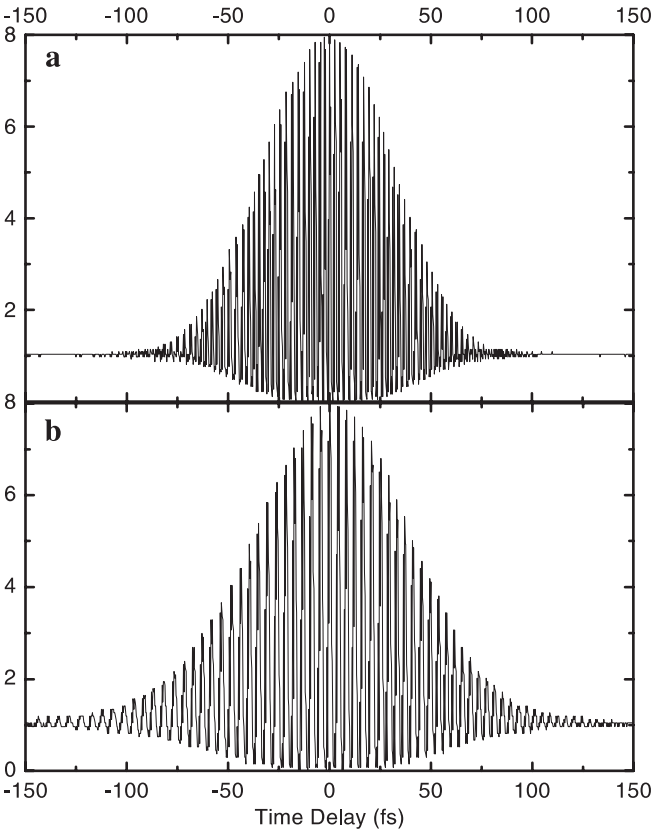

FIGURE 7 Fringe-resolved interferometric autocorrelation traces of the synchronized Ti:sapphire (**a**) and Cr:forsterite (**b**) lasers. The pulse durations were 43 ± 2 fs and 52 ± 1 fs with the assumption of a sech^2 shape, corresponding to the spectra centered around 820 nm and 1250 nm respectively

blocking the two SHG signals with a pinhole, we can accurately record the cross-correlation trace with a PMT and an oscilloscope.

Before the cross-correlation measurement between the Ti:sapphire and Cr:forsterite lasers, we first measured their pulse durations at the BBO crystal with the same configuration. Figure 7 shows the typical interferometric autocorrela-

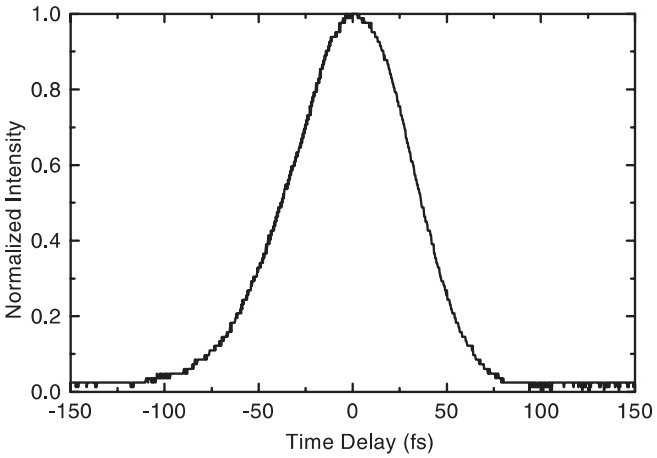

FIGURE 8 The cross-correlation trace between the Ti:sapphire and Cr:forsterite lasers. The measured width (FWHM) is 74 ± 2 fs within the experimental accuracy

tion traces. With careful calibration, we deduced both pulse widths of 43 ± 2 fs and 52 ± 1 fswith the assumption of a sech^2 shape, corresponding to the spectra centered at around 820 nm and 1250 nm respectively. Different to the autocorrelation, the cross-correlation measurement had some difficulty because of the delay matching of the two lasers (i.e. distance matching from the Ti:sapphire crystal to the beam splitter). Setting the distances as close as possible, we observed two alternate SFG signals at the central wavelength of around 495 nm by scanning the delay line via the PZT, which correspond to the forward and backward synchronized regimes started by shortening and lengthening the cavity length. We also found that the forward and backward synchronized regimes have a similar allowable range of cavity-length mismatch. Adjusting the length from the Ti:sapphire crystal to the output coupler T1 (or T2) enables us to observe the two types of SFG signal at the same delay range. By sweeping the delay line, we measured the typical cross-correlation trace as shown in Fig. 8. Using the same calibration of delay-time scale as the case of fringe-resolved autocorrelation, we deduced the width (FWHM) of the cross-correlation trace of 74 ± 2 fs within the experimental accuracy. Based on the pulse durations of the Ti:sapphire and Cr:forsterite lasers, we also calculated the theoretical value of 74 ± 2 fs with a sech^2 fit. The surprising coincidence between the two values infers that the two-color laser is synchronized with a timing jitter of only a few femtoseconds.

4 Conclusions

In summary, we successfully realized the stable synchronization between two independent femtosecond Ti:sapphire and Cr:forsterite lasers by crossing them inside the Ti:sapphire crystal. A long tolerance of cavity-length mismatch of 5 μm and a long-term synchronized operation over many hours were demonstrated. For the first time, our experiment demonstrated the unique towing effects in both repetition rates and wavelengths between the two lasers. Using a simple picture with the nonlinear coupling effect, we satisfactorily explained behaviors of the synchronizing process and gave a basis for detailed analysis in the future. Sliding prisms inside the cavities also enables us to tune the wavelengths of the two lasers independently under the synchronizing mode. Tuning the two central wavelengths around 820 nm and 1250 nm, we measured that the pulse durations were 43 ± 2 fs and 52 ± 1 fs respectively within the experimental accuracy. The calculated width (FWHM) of the cross-correlation trace coincides exactly with the measured value of 74 ± 2 fs, inferred that the two-color laser is synchronized with a timing jitter of only a few femtoseconds. The novel two-color femtosecond laser will not only supply an ideal tool for ultra-fast spectroscopy and frequency metrology, but also enable us to open a way to synchronize any different femtosecond KLM lasers.

ACKNOWLEDGEMENTS We gratefully acknowledge Zhigang Zhang for his early work on the Cr:forsterite laser. The authors also thank Masayuki Kakehata for the helpful discussion and appreciate the assistance of Hideyuki Takada, Kazuya Takasago and Shinji Ito. This research was conducted partially under the management of the Femtosecond Technology Research Association, which is supported by the New Energy and Industrial Technology Development Organization. Z. Wei also acknowledges partial support by the National Science Foundation of China under Grant No. 69878032.

REFERENCES

1 C. Chudoba, J.G. Fujimoto, E.P. Ippen, H.A. Haus, U. Morgner, F.X. Kärtner, V. Scheuer, G. Angelow, T. Tschudi: Opt. Lett. **26**, 292 (2001)
2 R. Ell, U. Morgner, F.X. Kärtner, J.G. Fujimoto, E.P. Ippen, V. Scheuer, G. Angelow, T. Tschudi, M.J. Lederer, A. Boiko, B. Luther-Davies: Opt. Lett. **26**, 373 (2001)
3 L.-S. Ma, R.K. Shelton, H.C. Kapteyn, M.M. Murnane, J. Ye: Phys. Rev. A **64**, 021 802(R) (2001)
4 D.E. Spence, W.E. Sleat, J.M. Evans, W. Sibbett, J.D. Kafka: Opt. Commun. **101**, 286 (1993)
5 S.A. Crooker, F.D. Betz, J. Levy, D.D. Awschalom: Rev. Sci. Instrum. **67**, 2068 (1996)
6 M.R.X. de Barros, P.C. Becker: Opt. Lett. **18**, 631 (1993)
7 D.R. Dykaar, S.B. Darack: Opt. Lett. **18**, 634 (1993).
8 J.M. Evans, D.E. Spence, D. Burns, W. Sibbett: Opt. Lett. **18**, 1074 (1993)
9 Z. Zhang, T. Yagi: Opt. Lett. **18**, 2126 (1993)
10 A. Leitenstorfer, C. Fürst, A. Laubereau: Opt. Lett. **20**, 916 (1995)
11 W. Shuicai, Z. Changjun, H. Junfang, Y. Hongru, X. Dong, H. Xun: Appl. Phys. B **68**, 211 (1999)
12 Z. Zhang, K. Torizuka, T. Itatani, K. Kobayashi, T. Sugaya, T. Nakagawa, H. Takahashi: Opt. Lett. **23,** 1465 (1998)
13 Z. Wei, Y. Kobayashi, Z. Zhang, K. Torizuka: Opt. Lett. **26**, 1806 (2001)
14 S.J. White, J.-M. Hopkins, M. Mazilu, A. Miller, W.H. Knox: Tech. Dig. CLEO 2000, CThB5, p. 395
15 C. Fürst, A. Leitenstorfer, A. Laubereau: IEEE J. Sel. Top. Quantum Electron. **2**, 473 (1996)